ASSESSMENT OF BLURRING EFFECT AND ITS ASSOCIATED FACTORS BY USING IMAGEJ: A MULTIPARAMETER DOUBLE HOLES CONTRAST-DETAIL PHANTOM STUDY

NUR FARAHANA PAUZI, MHSc.
DEPARTMENT OF DIAGNOSTIC IMAGING AND RADIOTHERAPY,
KULLIYYAH OF ALLIED HEALTH SCIENCES,
INTERNATIONAL ISLAMIC UNIVERSITY MALAYSIA,
25200 KUANTAN, PAHANG, MALAYSIA

ZAFRI AZRAN ABDUL MAJID, PhD (CORRESPONDING AUTHOR)
DEPARTMENT OF DIAGNOSTIC IMAGING AND RADIOTHERAPY,
KULLIYYAH OF ALLIED HEALTH SCIENCES,
INTERNATIONAL ISLAMIC UNIVERSITY MALAYSIA,
25200 KUANTAN, PAHANG, MALAYSIA
zafriazran@yahoo.com

WAN MUHAMAD NASUHA WAN HUSSIN, B. RADIOG. (HONS)
DEPARTMENT OF DIAGNOSTIC IMAGING AND RADIOTHERAPY,
KULLIYYAH OF ALLIED HEALTH SCIENCES,
INTERNATIONAL ISLAMIC UNIVERSITY MALAYSIA,
25200 KUANTAN, PAHANG, MALAYSIA

ABDUL HALIM SAPUAN, MSc.
DEPARTMENT OF DIAGNOSTIC IMAGING AND RADIOTHERAPY,
KULLIYYAH OF ALLIED HEALTH SCIENCES,
INTERNATIONAL ISLAMIC UNIVERSITY MALAYSIA,
25200 KUANTAN, PAHANG, MALAYSIA

MOHD ZULFAEZAL CHE AZEMIN, PhD
DEPARTMENT OF OPTOMETRY AND VISUAL SCIENCE,
KULLIYYAH OF ALLIED HEALTH SCIENCES,
INTERNATIONAL ISLAMIC UNIVERSITY MALAYSIA,
25200 KUANTAN, PAHANG, MALAYSIA

ABSTRACT

Introduction: X-ray is produced in form of divergent beam. The beam divergence results to blurring effect that influences image diagnosis. Thus, the blurring effect assessment should be enrolled within the quality control (QC) program of an imaging unit.

Method: this study is conducted by using multiparameter double holes contrast-detail (MDHCD) phantom to define the blurring effect and its associated factors which include the source-to-image receptor distance (SID), object thickness, and object distance from center. This study was conducted by exposing the phantom with x-ray where the factors were manipulated. ImageJ software was used to analyze the phantom images by plotting pixel intensity curves and measuring area under the curves (AUC) of two areas (area 1 and area 2).

Results: From the result, increased SID (750-1250-1750) mm, decreases the AUC reading (area 1; 415-328-306, area 2; 454-339-308) Pixel-per-millimeter (Ppmm). When object thickness increases (13-18-23) mm, AUC increases (area 1; 262-321-349, area 2; 274-333-386) Ppmm. Lastly, when the distance from center is increased (50-100-150) mm, AUC increases (area 1; 401-438-449, area 2; 459- 477-487) Ppmm.

Conclusion: In conclusion, the blurring effect is more prominent as the SID decreases and the object thickness and distance from center increase.

KEYWORDS: MDHCD phantom; Blurring effect; SID; X-ray beam divergence.

INTRODUCTION

Since the x-rays are created in the form of a beam, they propagate at different angle which contribute to a characteristic known as the divergent beam. It is due to x-ray comes from tiny source in the x-ray tube and propagates in divergence (Bontrager & Lampignano, 2010). Divergent x-ray beam gives several radiographic image appearances like magnification, distortion, and edge blurring. It creates a penumbra phenomenon which leads to the blurring effects. Image blur is actually an ill-appearance that is a misrepresentation of an object in an image which can degrade the image quality, whereby, almost all recorded detail is loss from the stripe or spread of the blur (Carlton, Adler, & Frank, 2006).

Basically, the penumbra results to blurring effect as the distance of structure is farther from the center of the collimated field. Extensively, the blurring effect may be related to the properties of SID which contributes to image distortion that deals with the scatter radiation and the photon intensity especially when it results to a low contrast image as stated in previous study, at the lowest contrast level, the blur shows its effect most evidently (Van Overveld, 1995). Thus, blurring effect that occurs due to divergent beam characteristic and signal-to-noise ratio (SNR) factor with respect to the characteristics of the structure being imaged within the collimated field is inevitable due to it is the nature of the beam itself.

In this study, the blurring effect is determined and analyzed by using a custom made radiographic QC phantom called Multiparameter Double Holes Contrast-Detail (MDHCD) phantom which is an extended function phantom from the commercialized contrast-detail (CD) phantom. MDHCD phantom is built using the same material used to develop the CD phantom but, the MDHCD phantom is constructed as a 3 dimensional (3D) phantom which takes it frontier to be utilized for more parameters of test as compared to CD phantom. The assessment that can be conducted using MDHCD phantom includes image displacement, angle of deviation, contrast-detail characteristics, and blurring effect. This research will be focused on the blurring effect assessment by using MDHCD phantom. The MDHCD phantom is more suitable to be used due to it can give the actual perception image of the location of the object within the phantom (Pauzi et al., 2014). Thus, it is very helpful to investigate how far the blurring effect has corrupted the image. Plus, the varying thickness and location of the components within the phantom can be related to the human anatomical structures which are different in size, position, and thickness. Blurring effect can give significant effect in radiographic image evaluation that may lead to misdiagnosis. Thus, this study is conducted in order to investigate how much the blurring would affect the visibility of radiographic images and the factors that may contribute to the blurring effect. The variables that are studied in this research are SID setting, object thickness, and object distance from center.

ImageJ has been widely used to perform various image processing and analysis. In this research, ImageJ is going to be utilized in calculating the pixel intensities of the MDHCD phantom image. The use of ImageJ is also intended to eliminate bias in evaluating the image blurring by human analyzer. Thus, ImageJ is used to analyze the image in this study where the MDHCD phantom is fabricated and utilized to acquire the image for analysis. In conclusion, this study is relevant to be performed as the blurring effect can actually influence the radiographic image evaluation which can result to misdiagnosis that certainly can harm the patients.

EXPERIMENTAL SET UP

Design of Multiparameter Double Holes Contrast-Detail (MDHCD) Phantom

An innovation from CD phantom designed to be used for four parameters assessment in accordance with the literatures consulted. The independent variables include image displacement assessment, detecting the shifting of anode stem, blurring analysis and contrast detail characteristic. For this reason, the experiment was accomplished by using the double holes acrylic block design of the MDHCD phantom since this type of design provides advantages to save time and cost reducing the number of experiments. Besides, the material used to build up this phantom which is acrylic gives the attenuation characteristics in almost the same with human soft tissues. Therefore, the result of this study is more clinical valid.

The clear acrylic is able to transmit the x-ray beam in regular thickness and it has same x-ray absorption coefficient as water. The colourless acrylic material has light transmittance of 92% and it has the density of 1.17-1.20 g/cm3. It is more resistant to thermal shock than glass while it has coefficient of thermal conductivity (k-factor) of 1.3 BTU/(Hr) (Sq. Ft) (°F/in) (0.19 w/m·K).

It is made of 25 acrylic blocks which are arranged together in a circular pattern to form three layers of a circular arrangement structure with one acrylic block positioned at the center of the phantom. The circular layers are referred as rims in which one rim holds eight acrylic blocks. From the design, there are eight radiated lines in which one line consists of three acrylic blocks projected from the center to the outermost acrylic block in one straight line of 150 mm in length. The angle between adjacent radiated lines is 45 degrees originated from the center of the phantom. The distance between two adjacent acrylic blocks in a radiated line is 50 mm.

All of the acrylic blocks are set up on a piece of square acrylic sheet with the dimension of 35 mm x 35 mm and 3 mm thick. Each acrylic block consists of double holes and double layers that contribute to its thickness. For this study, upper layer thickness of an acrylic block to be used is 3 mm and it is fixed for

the subsequent experiment. For the lower layer, the thickness is varied within 10 mm, 15 mm, and 20 mm which make the thickness of the acrylic block to become 13 mm, 18 mm, and 23 mm. As for the diameter of the double holes, the upper hole diameter is 3 mm and the lower hole diameter is 10 mm. The diameter of the acrylic block itself is 29 mm.

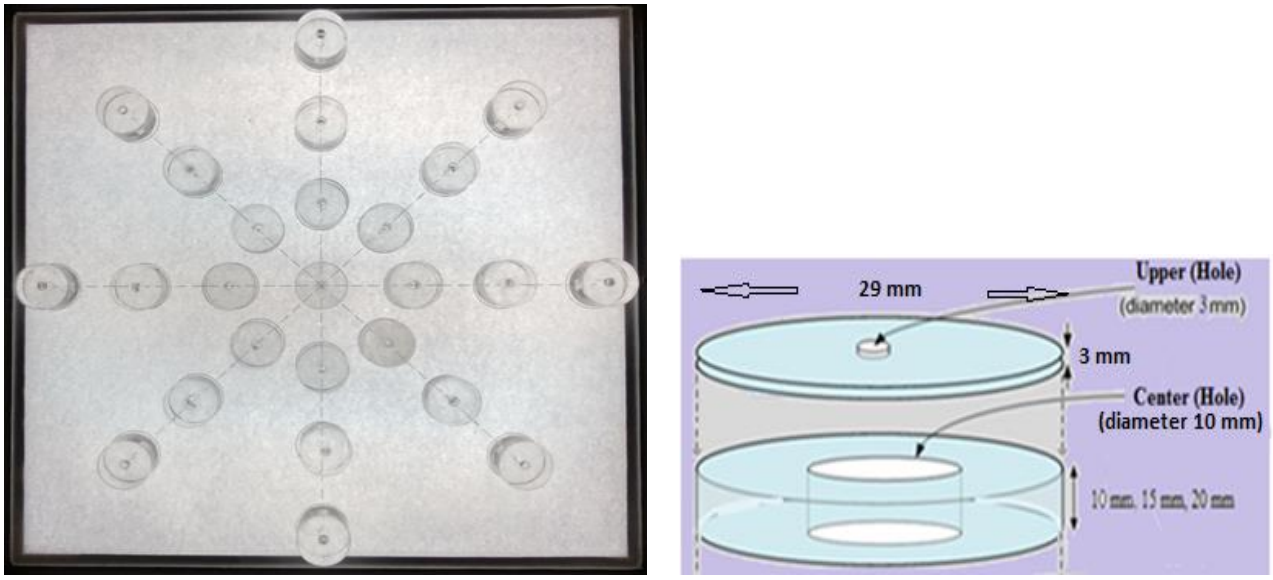

(a) (b)

Figure 1. Schematic diagram (a) superior view of MDHCD phantom; (b) double holes cylindrical acrylic block of MDHCD phantom.

Experimental Procedure

The MDHCD phantom was fabricated based on the design discussed earlier. Draft Sight software was used to geometrically sketch the base of the acrylic blocks position of the phantom on a plain paper. Then, the sketch was bound onto the surface of the acrylic sheet. The phantom was fabricated by positioning the double holes acrylic blocks on the sheet accordingly. For the first experiment, the MDHCD phantom that was used consists of 13 mm thickness acrylic blocks with 3 mm upper holes diameter and 10 mm lower hole diameter. Firstly, the Computed Radiography (CR) Imaging Plate (IP) of 14 × 17 inches was erased to discard any remnant image by using CR reader. Then, the IP was placed on the table top in crosswise orientation. Next, the MDHCD phantom was positioned on the IP and an anatomical marker was put at upper right side of the phantom in order to make sure the same phantom orientation was achieved when conducting the next experiment.

The SID value was set to 750 mm and the center of collimation field was adjusted to ensure that it was aligned with the center of the phantom. Then, the collimation was opened to 43 cm × 43 cm. The exposure was done in direct exposure and the broad focus was selected. As for the exposure setting, the kiloVoltage peak (kVp) value was 75 kV and the milliAmpere second (mAs) value was 4.0 mAs. After the experimental setup was done, the exposure was made and the data was collected. The experiment was repeated by changing the SID setting to 1250 mm followed by 1750 mm with the same MDHCD phantom thickness and hole diameter. Then, the experiment was repeated for different phantom thickness of 18 mm and followed by 23 mm. Each phantom thickness was exposed three times with the SID of 750 mm, 1250 mm, and 1750 mm respectively.

The images acquired were collected and analyzed by using ImageJ software to define the pixel intensities or gray value of double holes acrylic blocks. Each acrylic block image was cropped from the phantom and magnified to suit the analyzer preference. Next, a straight line was drawn crossing the acrylic block image and passing through the center of the acrylic block in zero degree. Then, a curve of pixel intensity or grey value versus distance was plotted base on the straight line propagation. After that, the reading of pixel intensities at 15 different designated points assigned to show the changes in pixel intensities on the image. The steps were repeated to analyze the other acrylic block images from the phantom. The result is determined by analyzing the curve and readings of pixel intensity or gray value over distance in pixel number of selected acrylic block images of respective parameter.

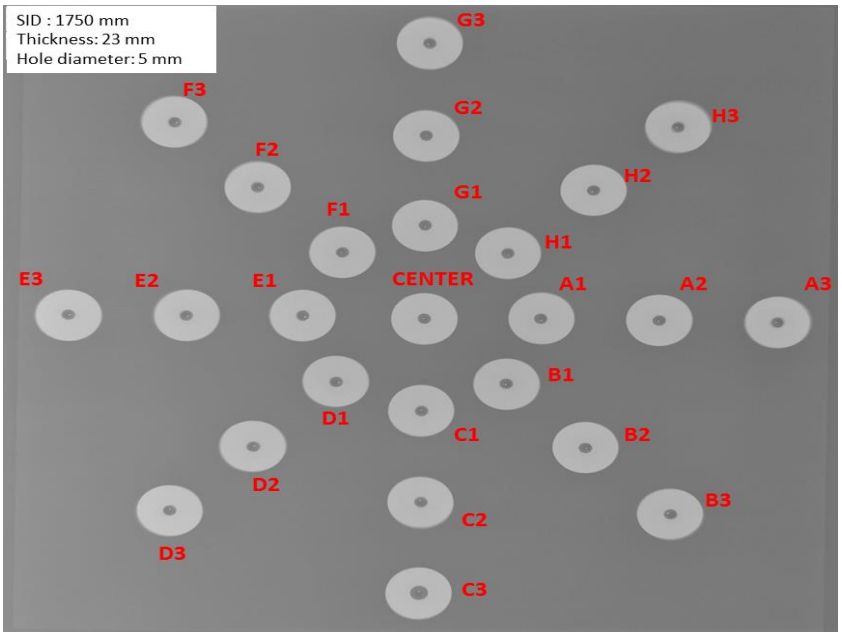

Figure 2. Labelling of double holes acrylic blocks of MDHCD phantom.

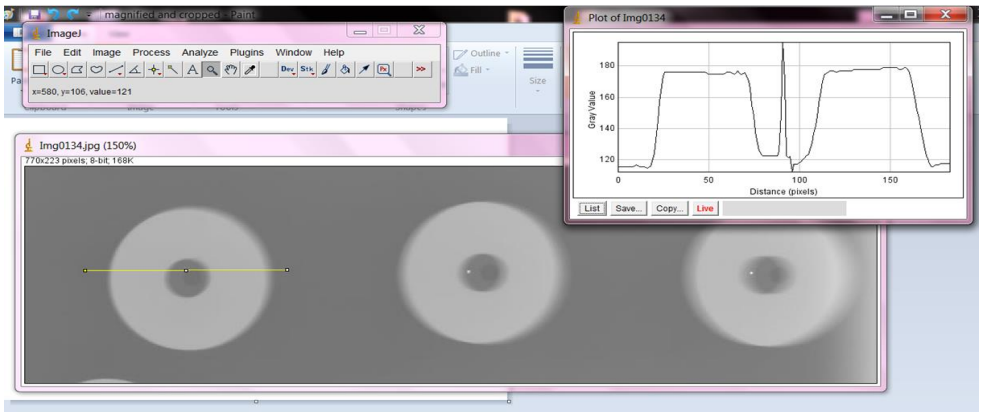

Figure 3. Plotting the curve as the straight line travelled.

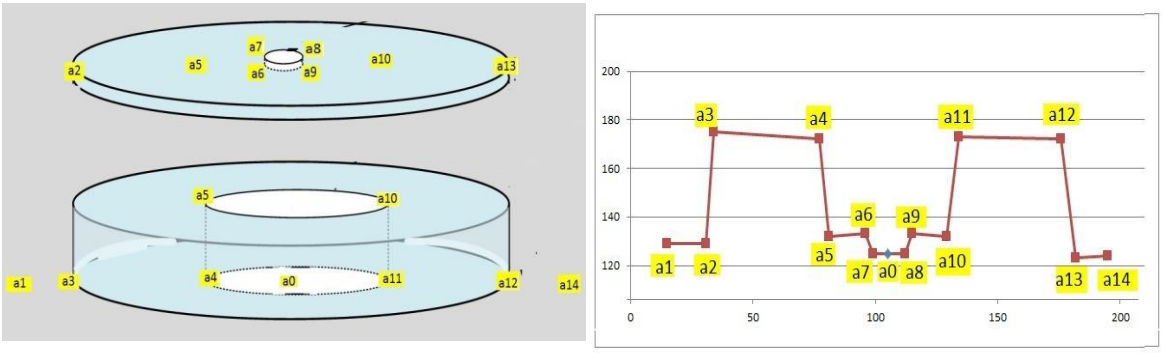

(a) (b)

Figure 4. (a) 15 designated points in double holes acrylic block; (b) 15 designated points in pixel intensity profile.

Results from three examinations were taken to show the role of SID in ruling the blurring effects. Those were examinations of MDHCD phantom in fixed acrylic block thickness, 18 mm (15 mm & 3 mm), in three manipulated SIDs, 750 mm, 1250 mm, and 1750 mm and it was obtained from A2 acrylic block images from the first radiated line (0 degree). The reason for taking the thickness of 18 mm and A2 (100 mm from center) acrylic block images as constants in this assessment was to average the blurring effects due to object thickness and blurring effects due to object distance from center respectively.

Table 1. Selected experiments done with respect to different SID settings.

		UPPER	UPPER	LOWER	LOWER
TEST	SID (mm)	Block height(mm)	Block diameter(mm)	Block height(mm)	Block diameter(mm)
1	750	3	3	10	10
2	1250	3	3	10	10
3	1750	3	3	10	10

4	750	3	3	15	10
5	1250	3	3	15	10
6	1750	3	3	15	10
7	750	3	3	20	10
8	1250	3	3	20	10
9	1750	3	3	20	10

The result to interpret the effect of object thickness on blurring was obtained by comparing the intensity value of A2 acrylic block of the first radiated line images of different thickness which was 13 mm (10 mm & 3 mm), 18 mm (15 mm & 3 mm), and 23 mm (20 mm & 3 mm) in a selected SID setting that was 1250 mm. The SID was kept to 1250 mm and A2 acrylic block is chosen in order to average the blurring effect due to SID changes and the distance of object from center which is 100 mm.

Table 2. Selected experiments done with respect to different double holes acrylic block thicknesses.

TEST	SID (mm)	UPPER Block height(mm)	UPPER Block diameter(mm)	LOWER Block height(mm)	LOWER Block diameter(mm)
1	750	3	3	10	10
2	1250	3	3	10	10
3	1750	3	3	10	10
4	750	3	3	15	10
5	1250	3	3	15	10
6	1750	3	3	15	10
7	750	3	3	20	10
8	1250	3	3	20	10
9	1750	3	3	20	10

The result for the assessment of the relationship between blurring effect and the distance of object from center was obtained from the image of double holes acrylic block from the first radiated line in 1250 mm SID setting, 18 mm block thickness, and different distances from center which are 50 mm (A1), 100 mm (A2), and 150 mm (A3). One experiment was selected and assessment on three different distance from center of double holes acrylic blocks image were done which are 50 mm (A1), 100 mm (A2), and 150 mm (A3).

Table 3. Selected experiment in assessing the effect of different distance of double holes acrylic blocks from center towards blurring effect for SID of 1250 mm.

TEST	SID (mm)	UPPER Block height(mm)	UPPER Block diameter(mm)	LOWER Block height(mm)	LOWER Block diameter(mm)
1	750	3	3	10	10
2	1250	3	3	10	10
3	1750	3	3	10	10
4	750	3	3	15	10
5	1250	3	3	15	10
6	1750	3	3	15	10
7	750	3	3	20	10
8	1250	3	3	20	10
9	1750	3	3	20	10

Steps in Assessing the Blurring Effect

From the curves and tables, the characteristics of blurring effect were examined. The area under the curve (AUC) was calculated by using ImageJ software at two areas of each double holes acrylic block image which are the area from the designated point of a2 to a3 (area 1) and from a12 to a13 (area 2). The results of AUC readings were compared in order to evaluate the blurring effect of those acrylic block images.

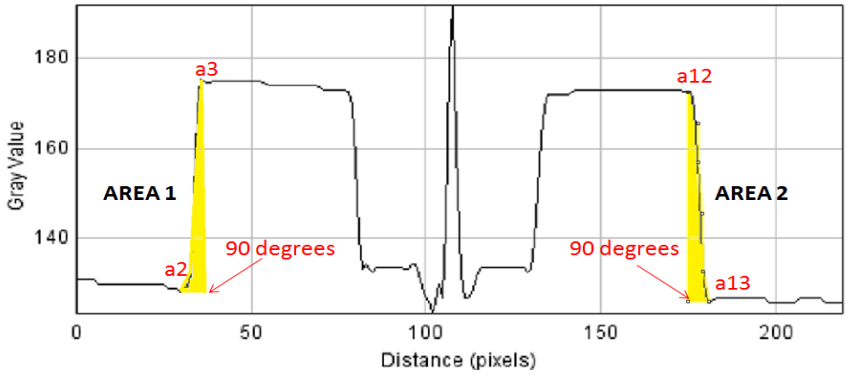

Figure 4: Measuring AUC by using ImageJ

Referring to Figure 4, the yellow shaded areas are the areas where the AUC were measured. The angle must be in 90 degrees to represent the real edge of the acrylic block. The calculation unit was calibrated to pixel-per-mm (Ppmm) and the measurement can be obtained directly as the parameter of area has been lined manually. The reading of the AUC represents the blurring effect that occurred at the edge of the double holes acrylic block. The AUC readings from each block are compared to quantisize the blurring effect.

RESULTS AND DISCUSSION

Comparison of the Result for Different SID Settings

Based on the curves and tables of the results of the A2 (100 mm from center) double holes acrylic block image in 18 mm block thickness with different SID settings, it is shown that the AUC is decreased as the SID setting increases in both areas. For area 1, the AUC reading for the image of 750 mm SID setting is 415 Ppmm and decreases to 328 Ppmm as the SID is increased to 1250 mm. Then, it decreases to 306 Ppmm as the SID setting is increased to 1750 Ppmm.

As for area 2, the AUC reading decreases from 454 Ppmm to 339 Ppmm to 308 Ppmm as the SID setting is increased from 750 mm to 1250 mm to 1750 mm respectively. This indicates that the blurring effect is getting low as the SID setting is getting high. Further, as compared between area 1 and area 2 for all three SIDs, it is noted that AUC 1 is always lower than AUC 2 which indicates the blurring effect is more prominent at area 2.

The increase in SID results to the angle of the beam spread out becomes less severe. As the source is moved farther, the x-rays become more parallel (Hammer, 2015). In other words, the beam divergence becomes less as the SID is increased in which reducing the effect of blurring due to penumbra.

Comparison of the Result for Different Thickness of Double Hole Acrylic Blocks

Based on the curves and tables of the results of the A2 double holes acrylic block image in 1250 SID setting, with different thicknesses, it is shown that the AUC is increased as the thickness increases in both areas. For area 1, the AUC reading for the image of 13 mm thickness is 262 Ppmm and increases to 321 Ppmm as the thickness is increased to 18 mm. Then, it increases to 349 Ppmm as the thickness is increased to 23 mm.

As for area 2, the AUC reading increases from 274 Ppmm to 333 Ppmm to 386 Ppmm as the thickness is increased from 13 mm to 18 mm to 23 mm respectively. This indicates that the blurring effect is more as the thickness is increased. Additionally, as compared between area 1 and area 2 for all three thicknesses, it is noted that AUC 1 is always lower than AUC 2 which indicates the blurring effect is more prominent at area 2.

The thickness of an object gives rise to blurring as the thickness is increased. When the thickness of an object increases, the more it can attenuate the x-ray photons. The increase in thickness also means the increase in depth of an object to be travelled by x-ray. Thus, during attenuation, the photons either become absorbed, loss energy, or change in direction in which when the photons had lose energy and changed the direction of propagation, scattering will be induced to be crafted into radiograph and causing blurring to occur. According to Fessler (2015), depth dependent magnification effect contributes to image distortion. It is an attempt to say that the depth or thickness of an object regulates the image resolution in which related to the blurring effect.

Plus, the increase in object thickness is related to the increase of object-to-image receptor-distance (OID) specifically the top surface of the object in which promotes the blurring effects by increasing the magnification. Previous study has mentioned that, magnification reduces as the subject is closer to the detector (Wei et al., 2013). Thus, if the subject is brought farther from the detector which is increasing the OID, magnification will be ushered and leads to blurring.

Comparison of the Result for Different Positions of Acrylic Block from the Center Point of the MDHCD Phantom at the SID of 1250 mm

Based on the curves and tables of the results of the double holes acrylic block image in 1250 SID settings, 18 mm thickness with different block distances from center which are 50 mm (A1), 100 mm (A2), and 150 mm (A3), it is shown that the AUC is increased as the distance increases in both areas. For area 1, the AUC reading for the image of 100 mm distance from center (A1) is 401 Ppmm

and increases to 438 Ppmm as the distance is increased to 100 mm (A2). Then, it increases to 449 Ppmm as the distance is increased to 150 mm.

As for area 2, the AUC reading increases from 459 Ppmm to 477 Ppmm to 487 Ppmm as the distance is increased from 50 mm to 100 mm to 150 mm respectively. This indicates that the blurring effect is increased as the distance of double holes acrylic block from the center is increased. Plus, as compared between area 1 and area 2 for all three locations, it is noted that AUC 1 is always lower than AUC 2 which indicates the blurring effect is more prominent at area 2.

Increased object distance from the center of the object that is positioned near the edge of the collimated field exhibits more blurring effect as compared to the object which is nearer to center. Factor that lead to this appearance is the reduction of energy and intensity of x-ray photons at the peripheral region or penumbra of a divergent x-ray beam. As the x-ray beam exited the x-ray tube and diverge, the energy and intensity of the x-ray photons turn to be higher at the central region and become lower at the peripheral region. It is can also be said that the beam is hardened at central region of the beam. As found in a recent study, change in transverse displacement of an object along with photons scattering are the explanation for the blur caused by object length (Wei et al., 2013). Thus, more scattering occurs at the peripheral region as compared to the central region that may lead to more blurring effect caused by the object that is situated at the peripheral region.

In addition, the role of the divergent beam in producing more blurring effect over the peripheral region of the collimated field can be further understood by observing the image displacement of an object as it is far from the center of x-ray beam. Recent research has suggested that, when the object is more distant from the x-ray beam center, image displacement increases (Pauzi et al., 2014). The image displacement indicates a failure in an image to represent the true object in which distortion or magnification occurs that is much related to the blurring effect as mentioned in a study, an anatomy image is being spread out over a larger area when magnification is raised (Hammer, 2015).

CONCLUSIONS

As observed from the result, the blurring effect is prominent as the SID setting is decreased and when the thickness of an object and the distance of an object from center are increased. It is also succeeded to acknowledge how the blurring effect can be induced by anode stem off-position. The divergent of x-ray beam is the major source of the blurring effect phenomenon (penumbra) while the SID setting, object thickness, and distance of an object to center are among the variables which determine the amount of blurring in an image. By using appropriate test tool which is the MDHCD phantom for experimental

procedure and ImageJ software to process and analyze the image outcome, the blurring effect can be defined and measured. It is hoped that, the MDHCD phantom will become one of the commercialized QC phantom tool in the future since it is convenience and reliable to be used not only to assess the blurring effect but also other parameters.

Plus, it is hoped that this study can be carried out further so that the blurring effect in medical images can be dealt with the right approach. Additionally, as the blurring effect cannot be avoided due to divergent x-ray beam, thus, a standard range of acceptability of blurring effect to present in a diagnostic image should be set.

ACKNOWLEDGEMENTS

The authors would like to express their gratitude to Department of Diagnostic Imaging & Radiotherapy, International Islamic University Malaysia Pahang for providing laboratory facilities and financial assistance from Radtec Enterprise.

REFERENCES

Bontrager, K. L., & Lampignano, J. P. (2010). Textbook of radiographic positioning and related anatomy. St. Louis, MO: Elsevier/Mosby.

Carlton, R. R., Adler, A. M., & Frank, E. (2006). Principles of radiographic imaging. Clifton Park, NY: Thomson Delmar Learning.

Fessler, J. X-ray source considerations. (n.d.). Retrieved April 18, 2015, from http://web.eecs.umich.edu/~fessler/course/516/l/c4-source.pdf

Hammer, M. X-Ray Physics: Magnification and Collimation in Radiography. (n.d.). Retrieved March 20, 2015, from http://xrayphysics.com/radio.html

Pauzi, N. F., Majid, A., Azran, Z., Sapuan, A. H., Azemin, C., Zulfaezal, M., & Junet, L. K. (2014). Assessment of Double Hole Contrast Detail Phantom for Image Displacement Evaluation. In Applied Mechanics and Materials (Vol. 661, pp. 168-175). Trans Tech Publications.

Van Overveld, I. M. (1995). Contrast, noise, and blur affect performance and appreciation of digital radiographs. Journal of digital imaging, 8(4), 168-179.

Wei, T., Yang, G., Long, J., & Shi, J. (2013). Image blur in high energy proton radiography. *Chinese Physics C, 37*(6), 068201.